iScience

CellPress
OPEN ACCESS

Article

# Evolutionarily Conserved Roles for Apontic in Induction and Subsequent Decline of Cyclin E Expression

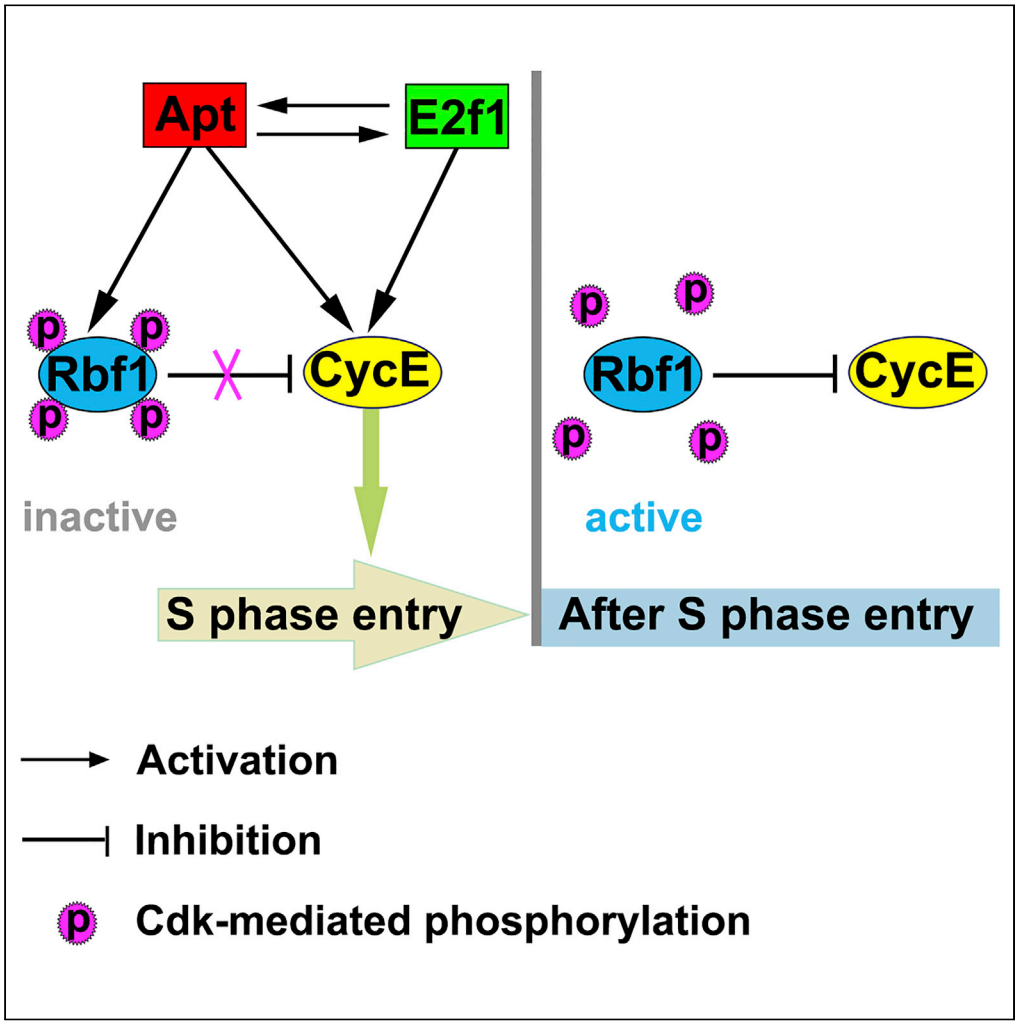


Xian-Feng Wang, Jin-Xiao Liu, Zhi-Yuan Ma, ..., Emiko Suzuki, Qing-Xin Liu, Susumu Hirose

liuqingxin@sdau.edu.cn (Q.-X.L.)
shirose@nig.ac.jp (S.H.)

## HIGHLIGHTS

Mutual activation of *apt* and *e2f1* promotes rapid induction of CycE at S phase entry

Apt also up-regulates Rbf1, but Rbf1 is inactivated through phosphorylation by Cdk2

After initiation of S phase, Rbf1 becomes active and represses *cycE*

Apt governs both induction and subsequent repression of *cycE*

Wang et al., iScience *23*, 101369
August 21, 2020 
https://doi.org/10.1016/j.isci.2020.101369

iScience

CellPress
OPEN ACCESS

Article

# Evolutionarily Conserved Roles for Apontic in Induction and Subsequent Decline of Cyclin E Expression

Xian-Feng Wang,[1,2] Jin-Xiao Liu,[2] Zhi-Yuan Ma,[2] Yang Shen,[2] Hao-Ran Zhang,[2] Zi-Zhang Zhou,[2] Emiko Suzuki,[1] Qing-Xin Liu,[2,*] and Susumu Hirose[1,3,*]

## SUMMARY

**Cyclin E is a key factor for S phase entry, and deregulation of Cyclin E results in developmental defects and tumors. Therefore, proper cycling of Cyclin E is crucial for normal growth. Here we found that transcription factors Apontic (Apt) and E2f1 cooperate to induce *cyclin E* in *Drosophila*. Functional binding motifs of Apt and E2f1 are clustered in the first intron of *Drosophila cyclin E* and directly contribute to the *cyclin E* transcription. Knockout of *apt* and *e2f1* together abolished Cyclin E expression. Furthermore, Apt up-regulates Retinoblastoma family protein 1 (Rbf1) for proper chromatin compaction, which is known to repress *cyclin E*. Notably, Apt-dependent up-regulation of Cyclin E and Rbf1 is evolutionarily conserved in mammalian cells. Our findings reveal a unique mechanism underlying the induction and subsequent decline of Cyclin E expression.**

## INTRODUCTION

As a key factor for S phase entry, Cyclin E (CycE) is crucial for both mitotic and endocycling cells (Dulic et al., 1992; Knoblich et al., 1994; Lilly and Spradling, 1996). Previous studies have shown that transcription factor E2f, a heterodimer of E2f1 and Dp, plays an important role in *cycE* expression in normal cell cycle and endocycle (De Veylder et al., 2002; Duronio et al., 1995; van den Heuvel and Dyson, 2008; Zielke et al., 2011). However, *Drosophila e2f1* null mutant can survive to the third-instar larval stage and residual S phase occurs in the mutant cells (Duronio et al., 1998; Royzman et al., 1997), suggesting an involvement of another transcription factor in S phase entry.

One candidate for such factor is Apt. *Drosophila* Apt (also termed Trachea defective, Tdf) is a DNA-binding transcription factor that is involved in the development of multiple organs and tissues, such as tracheae, head, heart, ovary, stem cell, nervous system, and imaginal discs (Eulenberg and Schuh, 1997; Gellon et al., 1997; Lie and Macdonald, 1999; Liu et al., 2003, 2014; Monahan and Starz-Gaiano, 2016; Shen et al., 2018; Starz-Gaiano et al., 2008; Su et al., 1999; Wang et al., 2017). We have found that Apt directly regulates the expression of *cycE* during the development of imaginal discs (Liu et al., 2014; Wang et al., 2017). Therefore, Apt might participate in the expression of *cycE* in other tissues also. Besides, Apt can suppress tumor metastasis, and the human homolog of Apt, FSBP, is a cancer-related factor (Lau et al., 2010; Woodhouse et al., 2003).

Although CycE is crucial for S phase entry, it should decrease subsequently for progression of the cell cycle. Rbf1 is a key player in the decline of CycE expression (Cayirlioglu et al., 2003; Korenjak et al., 2012; van den Heuvel and Dyson, 2008; Weng et al., 2003). During S phase entry, Rbf1 is inactivated by phosphorylation with Cyclin-dependent kinase 2 (Cdk2) but becomes active by de-phosphorylation after initiation of S phase (Du et al., 1996; Edgar and Orr-Weaver, 2001; van den Heuvel and Dyson, 2008). The activated Rbf1 binds to E2f1 and also forms another complex containing E2f2 and Dp to repress E2f1-target genes including *cycE* and many other genes (Cayirlioglu et al., 2003; Korenjak et al., 2012; van den Heuvel and Dyson, 2008; Weng et al., 2003). Retinoblastoma protein (Rb), a mammalian counterpart of Rbf1, promotes chromatin compaction for transcriptional silencing by interaction with chromatin regulators such as histone deacetylases and histone methyltransferases (Brehm et al., 1998; Nielsen et al., 2001; Talluri and Dick, 2012). Therefore, Rbf1 is also expected to participate in chromatin compaction for silencing.

[1]Department of Gene Function and Phenomics, National Institute of Genetics, 1111 Yata, Mishima City, Shizuoka 411-8540, Japan

[2]State Key Laboratory of Crop Biology, College of Life Sciences, Shandong Agricultural University, Tai'an, Shandong 271018, China

[3]Lead Contact

*Correspondence: liuqingxin@sdau.edu.cn (Q.-X.L.), shirose@nig.ac.jp (S.H.)

https://doi.org/10.1016/j.isci.2020.101369

Here we provide evidence that both *Drosophila* Apt and mouse FSBP play important roles in the induction of CycE and up-regulation of Rbf1 for proper chromatin compaction. Mechanistically, we showed that Apt and E2f1 mutually activate the expression of each other to induce *cycE* for S phase entry in the salivary gland. Furthermore, we observed that the binding motifs of Apt and E2f are clustered in the first intron of *cycE*. Based on the results of chromatin immunoprecipitation (ChIP) and transgenic reporter assays, we found direct contribution of the Apt-binding sites and the E2f1-binding sites to the *cycE* transcription in the salivary gland. Moreover, we also found that Apt up-regulates Rbf1 to direct proper chromatin compaction for transcriptional silencing. Finally, we demonstrated evolutionary conservation of these mechanisms in mammalian cells.

## RESULTS

### Apt and E2f1 Activate Expression of Each Other

To investigate the function of Apt in endoreplication of the salivary gland, we first compared the expression of Apt and E2f1 proteins by immunostaining (Figure 1A). Endocycle in the salivary gland proceeds asynchronously, and hence each cell resides in various phases of endocycle. E2f1 peaks at S phase entry and declines after initiation of S phase (Zielke et al., 2011). According to the oscillation of E2f1 during endocycle, some cells expressed E2f1 strongly, whereas other cells expressed weakly. Intriguingly, we noticed that the expression of Apt exhibits a similar pattern as that of E2f1. The observed tight correlation between the levels of Apt and E2f1 proteins suggests almost-synchronous oscillation of Apt and E2f1 during endocycle.

As Apt and E2f1 are transcription factors, the strong correlation between the levels of Apt and E2f1 could be due to the interdependence of the *apt* and *e2f1* expression. To test the possibility, we analyzed mRNA levels of *apt* and *e2f1* in the salivary gland by RT-qPCR. To compare the mRNA levels among samples with different genome dosages, each mRNA level was normalized to that of β-tubulin mRNA. RNAi knockdown of *e2f1* using a *dpp-GAL4* driver (Figure S1A) decreased the expression of *apt*, and vice versa (Figure 1B). Furthermore, the expression of Apt and E2f1 proteins were dependent on each other (Figure S1B). These data demonstrate mutual activation of *apt* and *e2f1*. The positive feedback between *apt* and *e2f1* would support their rapid and robust transaction. To examine whether these activations are direct or not, we searched for E2f1- and Apt-binding motifs in the *apt* or *e2f1* promoter. E2f1-binding sites were found in the *apt* promoter region, suggesting that E2f1 might directly activate *apt* transcription. We used the 1.5-kb promoter region containing the E2f1-binding sites (Figure S2) to verify this possibility through transgenic reporter assays. As we expected, wild-type reporter gene was expressed in the salivary gland (Figure 1C), whereas the expression level of the reporter gene significantly decreased in the E2f1-binding site mutant line (Figures 1C and 1D). These results demonstrate that E2f1 can directly activate *apt* transcription in the salivary gland. Because the Apt-binding site was not found in the *e2f1* promoter region, the *apt*-mediated activation of *e2f1* might be indirect.

### Both Apt and E2f1 Are Required for CycE Expression and Endoreplication

Considering the tight correlation between the expression of Apt and E2f1, it is most likely that Apt is involved in endocycle together with E2f1. To test the possibility, we induced *apt* null mutant clones in embryonic salivary glands where cells still undergo mitosis and observed the glands at the third-instar larval stage after many rounds of endoreplication in control cells. Compared with control cells, *apt*-knockout cells showed obvious decrease in DAPI fluorescence (Figures 2A and 2B). The decreased DAPI fluorescence indicates the role for Apt in endoreplication. In addition to the decreased DAPI staining, loose chromatin appearance was observed in *apt*-mutant clone cells (Figure 2A). We will refer to the phenotype in the later section.

In agreement with the previous studies (De Veylder et al., 2002; Duronio et al., 1995; van den Heuvel and Dyson, 2008; Zielke et al., 2011), knockdown of *e2f1* decreased the expression of *cycE* in the salivary gland (Figure 1B). Furthermore, knockdown of *apt* also reduced the expression of *cycE*. Having established that both E2f1 and Apt are *cycE* activators, we compared the DNA content and CycE protein level among control cells, *apt*-knockout cells, *e2f1*-knockout cells, and *apt*- and *e2f1*-double knockout cells. The DNA content decreased clearly in *apt*- or *e2f1*-knockout clone cells (Figures 2A, 2B, 2D and 2H). Double knockout of *apt* and *e2f1* completely blocked endoreplication (Figures 2E, 2E′ and 2H). Knockout of either *apt* or *e2f1* significantly decreased the CycE expression, but residual CycE protein was still detectable (Figures 2C and 2F). Upon double knockout of *apt* and *e2f1*, the expression level of CycE reduced below the

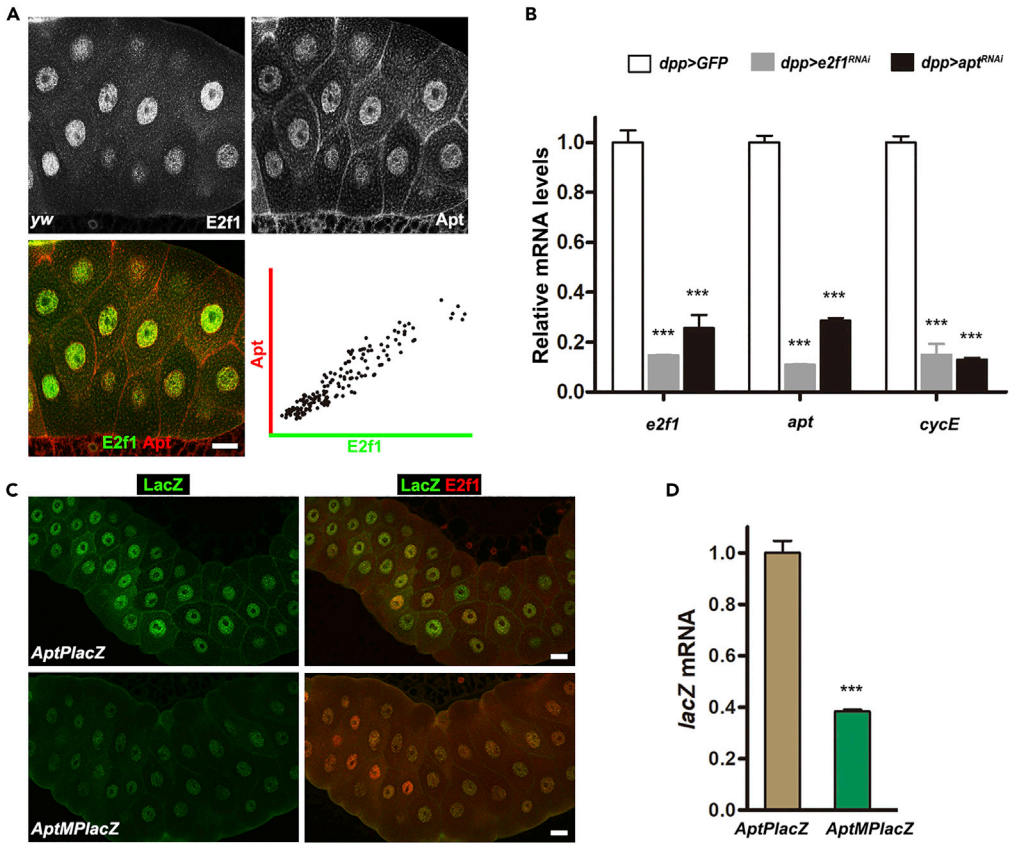


**Figure 1. Apt and E2f1 Up-regulate Each Other in the Salivary Gland**

(A) Expression of Apt and E2f1 at 72–84 h after egg laying (AEL). Each picture is the same single focal plane image of the salivary gland obtained with a confocal microscope. n = 16 with all samples showing the represented phenotype. Scale bar, 20 μm. The graph shows the correlation between Apt and E2f1 protein levels in each cell. n = 177. $R^2$ (coefficient of determination) = 0.89.

(B) RT-qPCR assays for expression of *e2f1*, *apt*, and *cycE* mRNAs. The glands were prepared from early third-instar larvae. Data were average ± SD relative to the *dpp* > *GFP* mRNA level. *dpp* > *GFP* samples were normalized to 1. ***p < 0.001 (Student's t test).

(C) Transgenic reporter assays for *apt* transcription. The reporter *AptPlacZ* (*apt* promoter region with wild-type E2f1-binding motifs) showed an expression pattern similar to the endogenous E2f1 expression. n = 8 with all samples showing the represented phenotype. *AptMPlacZ* (base substitutions in the E2f1-binding motifs in the *apt* promoter region) showed significantly decreased LacZ expression. n = 5 with all samples showing the represented phenotype. Scale bars, 20 μm.

(D) RT-qPCR assays for *lacZ* mRNA levels from AptPlacZ or AptMPlacZ. Data were average ± SD relative to the mRNA level of AptPlacZ. ***p < 0.001 (Student's t test).

See also Figures S1 and S2.

detection limit (Figure 2G). These data collectively demonstrate that both Apt and E2f1 are required for proper CycE expression and endoreplication in the salivary gland.

## Apt and E2f1 Can Directly Activate *cycE* Transcription

As Apt and E2f1 activate the expression of each other and both Apt and E2f1 are required for the CycE expression, effect of *e2f1* null mutation on the CycE expression is a combination of a direct effect due to the absence of E2f1 and an indirect effect due to the reduced Apt level. To address the direct contribution of Apt or E2f1 to *cycE* transcription, we focused on *cis*-regulatory elements of *cycE*. Expression of *cycE* is regulated by complex tissue-specific *cis*-elements (Jones et al., 2000). Although *cis*-elements for the expression in the salivary gland have not been reported, we found a clustering of two adjacent E2f1-binding motifs and four Apt-binding motifs in the first intron of *cycE* (Figure 3A). To test whether Apt or E2f1

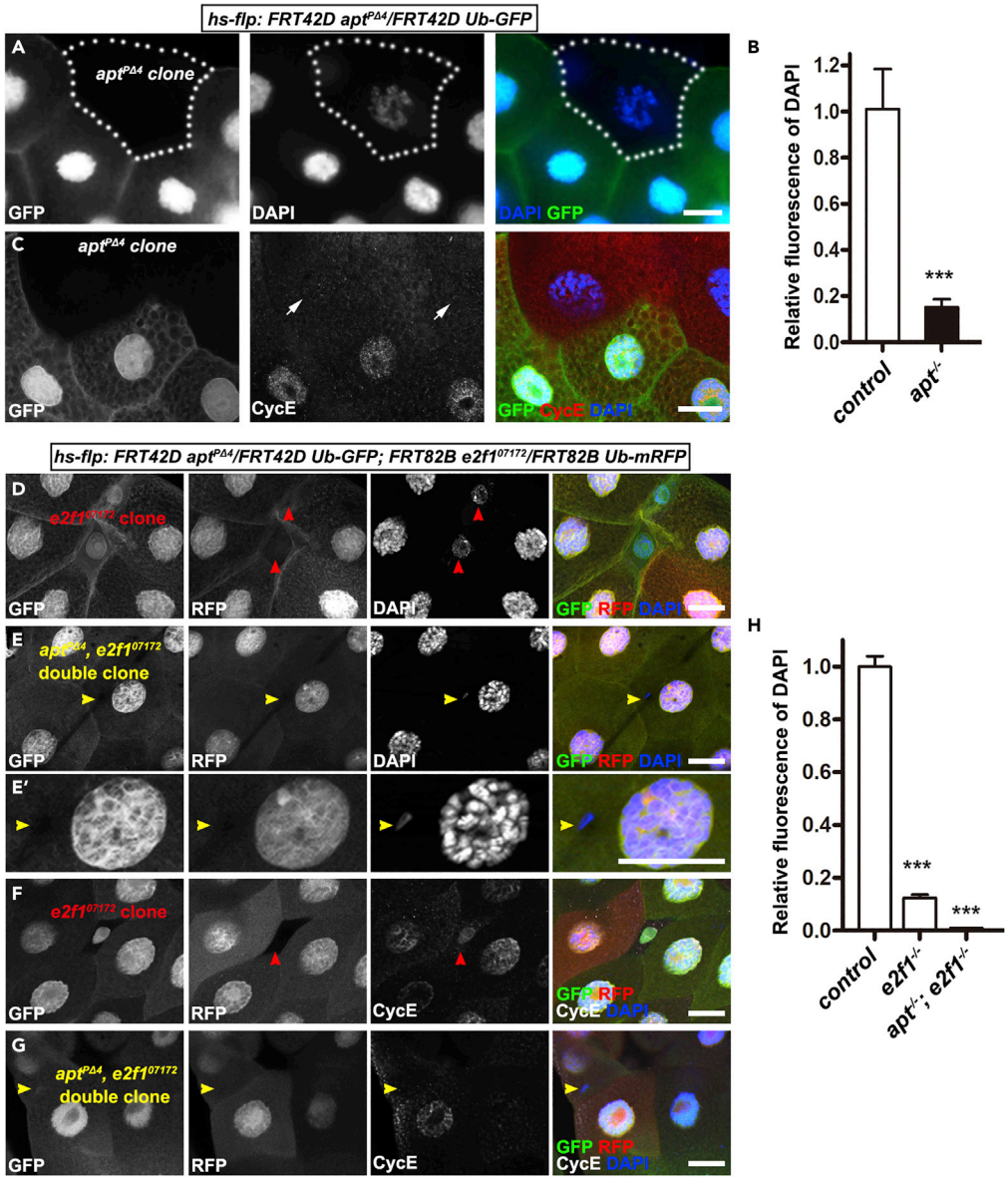


**Figure 2. Apt Is Required for Endoreplication and CycE Expression in the Salivary Gland**

(A) An *apt*-mutant clone (marked by white dotted lines) was stained with DAPI. n = 12 with all samples showing the represented phenotype. Scale bar, 20 μm.

(B) Quantification of DAPI fluorescence from *apt*-mutant clone cells and neighboring control cells. Data were presented as mean ± SD. n = 4 cells for *apt*-mutant clones and 10 cells for control. ***$p < 0.001$ versus the control (Student's t test).

(C) Immunofluorescence staining with anti-CycE antibody and DAPI in *apt*-mutant clones. Arrows show reduced expression of CycE in *apt*-mutant clones. n = 11 with all samples showing the represented phenotype. Scale bar, 20 μm.

(D) *e2f1*-knockout cells (marked by red arrowheads) showed lower ploidy. n = 7 with all samples showing the represented phenotype. Scale bar, 20 μm.

(E) An *apt*- and *e2f1*-double knockout cell (marked by yellow arrowheads) showed almost no endoreplication. n = 4 with all samples showing the represented phenotype. Scale bar, 20 μm.

(E′) Close-up image around the yellow arrowhead in (E). Scale bar, 20 μm.

(F) CycE was decreased but still detectable in an *e2f1*-mutant cell (marked by red arrowheads). n = 4 with all samples showing the represented phenotype. Scale bar, 20 μm.

(G) *apt*- and *e2f1*-double mutant cell (marked by yellow arrowheads) abolished CycE expression. n = 3 with all samples showing the represented phenotype. Scale bar, 20 μm.

**Figure 2. *Continued***

(H) Quantification of DAPI fluorescence in *e2f1*-mutant clone cells, *apt-e2f1*-double mutant clone cells, and neighboring control cells. Data were presented as mean ± SD. n = 4 cells for control, 3 cells for *e2f1*-mutant clone, and 3 cells for *apt-e2f1*-double mutant clone. ***p < 0.001 versus the control (Student's t test). See also Table S4.

binds to these motifs, we carried out ChIP experiments using Apt or E2f1 antibodies. The ChIP data clearly showed that Apt and E2f1 bind to the corresponding motifs (Figures 3B and 3C). Consistently, RNAi knockdown of *apt* prominently reduced the occupancies of Apt on the Apt motifs (Figure 3B). We then assessed the functional activities of these sites by transgenic reporter assays (Figures 3D and S3A). Control reporter carrying the 3-kb wild-type *cycE* region (*cycEPlacZ*) expressed LacZ in the salivary gland. Compared with the control, the LacZ expression decreased but was still detectable in E2f1-binding site mutation line (*E2f1BSMPlacZ*). Simultaneous disruption of the E2f1- and Apt-binding sites (*E2f1BSM* + *AptBSMPlacZ*) virtually abolished the reporter gene expression. Furthermore, the LacZ expression in *E2f1BSMPlacZ* reduced significantly upon RNAi knockdown of *apt* compared with non-RNAi control (Figure S3B). These data demonstrate that Apt and E2f1 can directly activate the *cycE* transcription. These data also indicate that both the Apt- and E2f1-binding sites are required for the normal level of *cycE* transcription.

The 3-kb regulatory element of *cycE* (termed I element here) is different from the 4-kb region (termed U element) that governs the *cycE* expression in the eye and wing discs (Liu et al., 2014; Wang et al., 2017). The I element is within the first intron, whereas the U element is immediately upstream of the start site of the *cycE* transcript A (Thurmond et al., 2019) (Figure S4A). E2f1-binding sites are present in the I element but not in the U element. To test the specificity of the cis-regulatory region, we checked the reporter activity of the I element in the eye disc. The I element failed to reproduce the complete expression pattern of CycE in the eye disc (Figure S4B). These results further support the tissue-specific regulation of *cycE* (Jones et al., 2000).

## Apt Up-regulates Rbf1 and Directs Proper Chromatin Compaction

*e2f1* mutant cells induced in the salivary gland displayed small nuclei with low DNA content (Figure 2D). This is exactly expected from the reduced endoreplication. By contrast, nuclei of *apt* mutant cells were abnormal. Despite the reduced level of endoreplication, the size of nuclei in the *apt* mutant clone cells was comparable to that of control cells (Figure 2A). The ratio of nuclear size to DNA content was ~6.5 times higher in *apt*-mutant cells than that in control cells (Figure 4A). A higher-magnification image of *apt* mutant nuclei exhibited intra-chromosomal chromatin de-compaction and large inter-chromosomal spaces compared with control nuclei (Figure S5). As the loose chromatin is associated with increased transcription activity, loss of *apt* function would induce de-repression of multiple genes. Indeed, *apt*-knockout cells exhibited many signals of transcribing RNA polymerase II, under the conditions where the signals were barely detectable in control cells (Figure 4B). Then, what is a global repressor that governs the silencing of many genes in the downstream of Apt? One candidate is Rbf1, because it forms a complex with E2f1 and another complex including E2f2 and Dp to repress E2f-target genes and many other genes (Cayirlioglu et al., 2003; Korenjak et al., 2012; van den Heuvel and Dyson, 2008; Weng et al., 2003). Consistent with this idea, we observed large nuclei with de-compacted chromatin upon RNAi knockdown of *rbf1* (Figure 4C). Therefore, it is possible that Apt up-regulates *rbf1*, and hence the *apt* mutant cells exhibit large nuclei with de-compacted chromatin. To test the possibility, we analyzed the expression of *rbf1* in the salivary gland by RT-qPCR. As shown in Figure 4D, we observed a significant reduction in the expression of *rbf1* and *e2f2* upon RNAi knockdown of *apt* leaving the *dp* expression unchanged. We also examined the expression of Rbf1 protein in *apt*-knockout or *apt*-overexpressing cells. Compared with control cells, *apt*-mutant clone cells showed decreased expression of Rbf1 protein, whereas *apt*-overexpressing cells exhibited highly compact chromatin with increased Rbf1 protein levels (Figures 4E and 4F). Consistently, we observed de-repression of Rbf1-target genes, such as *CG4679*, *gigas*, *diap3,* and *Ipp* upon knockdown of *apt* (Figure 4D). Importantly, overexpression of Rbf1 suppressed chromatin de-compaction upon RNAi knockdown of *apt* (Figure 4G). Based on these results, we reasoned that the nuclear defects in the *apt*-knockout cells are due to release from Rbf1-mediated chromatin compaction and de-repression of many Rbf1-target genes.

There exists a single Apt-binding motif at 156 nucleotides upstream of the transcription start site of *rbf1*. ChIP assays showed occupancy of Apt on the motif (Figure 4H). These data suggest that *rbf1* is a direct target of Apt.

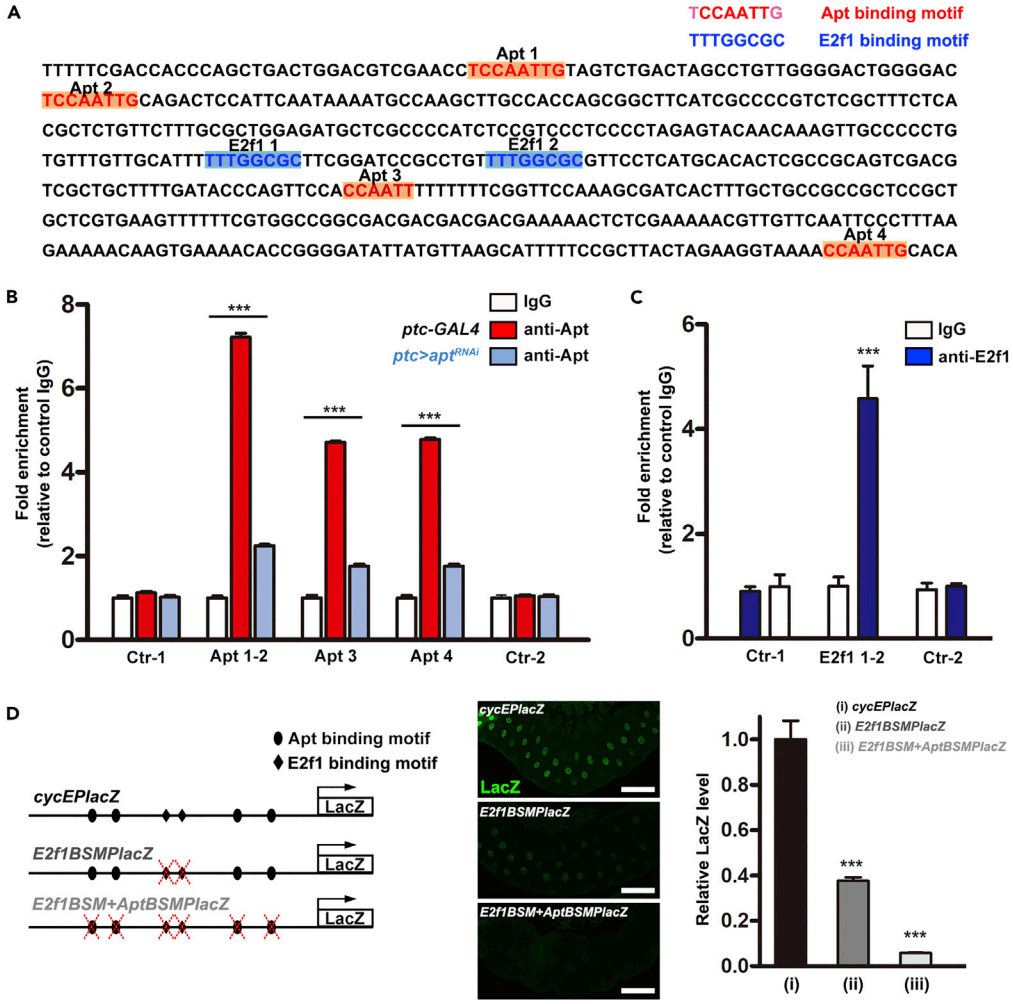


**Figure 3. Both Apt- and E2f1-Binding Sites Are Required for Normal Level of *cycE* Transcription**

(A) Clustering of Apt- and E2f1-binding motifs in the first intron of *cycE*. Apt-binding motifs and E2f1-binding motifs are indicated in red and blue, respectively.

(B and C) ChIP assays revealed occupancy of Apt (B) or E2f1 (C) at each binding motif. ChIP-qPCR was performed using antibodies against Apt (B) or E2f1 (C). Control regions of the anti-Apt antibody ChIP were set around 1.2 kb upstream of the Apt motif 1 (Ctr-1) and around 1.2 kb downstream of the Apt motif 4 (Ctr-2). Control regions of the anti-E2f1 antibody ChIP were set around 1.2 kb upstream of the E2f1 motif 1 (Ctr-1) and around 1.4 kb downstream of the E2f1 motif 2 (Ctr-2). Data were presented as mean ± SD. n = three biological replicates. ***$p < 0.001$ (Student's t test) between *ptc-GAL4* and control IgG or between *apt*RNAi and control *ptc-GAL4* in (B) and versus control IgG in (C).

(D) Reporter assays for contribution of Apt- and E2f1-binding motifs to *cycE* transcription. The left panel shows strategy of the transgenic reporter assays. Middle panel: The wild-type reporter (*cycEPlacZ*) displayed clear LacZ expression. n = 16 with all samples showing the represented phenotype. The E2f1-binding motif's mutant reporter (*E2f1BSMPlacZ*) exhibited reduced LacZ expression. n = 11 with all samples showing the represented phenotype. The reporter of Apt- and E2f1-binding motif's mutant (*E2f1BSM + AptBSMPlacZ*) almost abolished the LacZ expression. n = 8 with all samples showing the represented phenotype. Scale bars, 100 μm. Right panel: Quantification of the LacZ expression. Data were mean ± SD relative to the level of *cycEPlacZ*. n = 23 for *cycEPlacZ*, 20 for *E2f1BSMPlacZ*, and 29 for *E2f1BSM + AptBSMPlacZ*. ***$p < 0.001$ (Student's t test). See also Figures S3 and S4.

## Apt Up-regulates Rbf1 Also in Mitotic Cycling Cells

So far, we demonstrate the roles for Apt in the induction of CycE and chromatin compaction for silencing in endocycling salivary gland cells. Then, how is the situation in mitotic cycling cells? We have shown that Apt activates the *cycE* expression for S phase entry in imaginal disc cells undergoing mitotic cycles (Liu et al., 2014; Wang et al., 2017). This led us to examine whether Apt up-regulates Rbf1 also in the wing disc. Strong

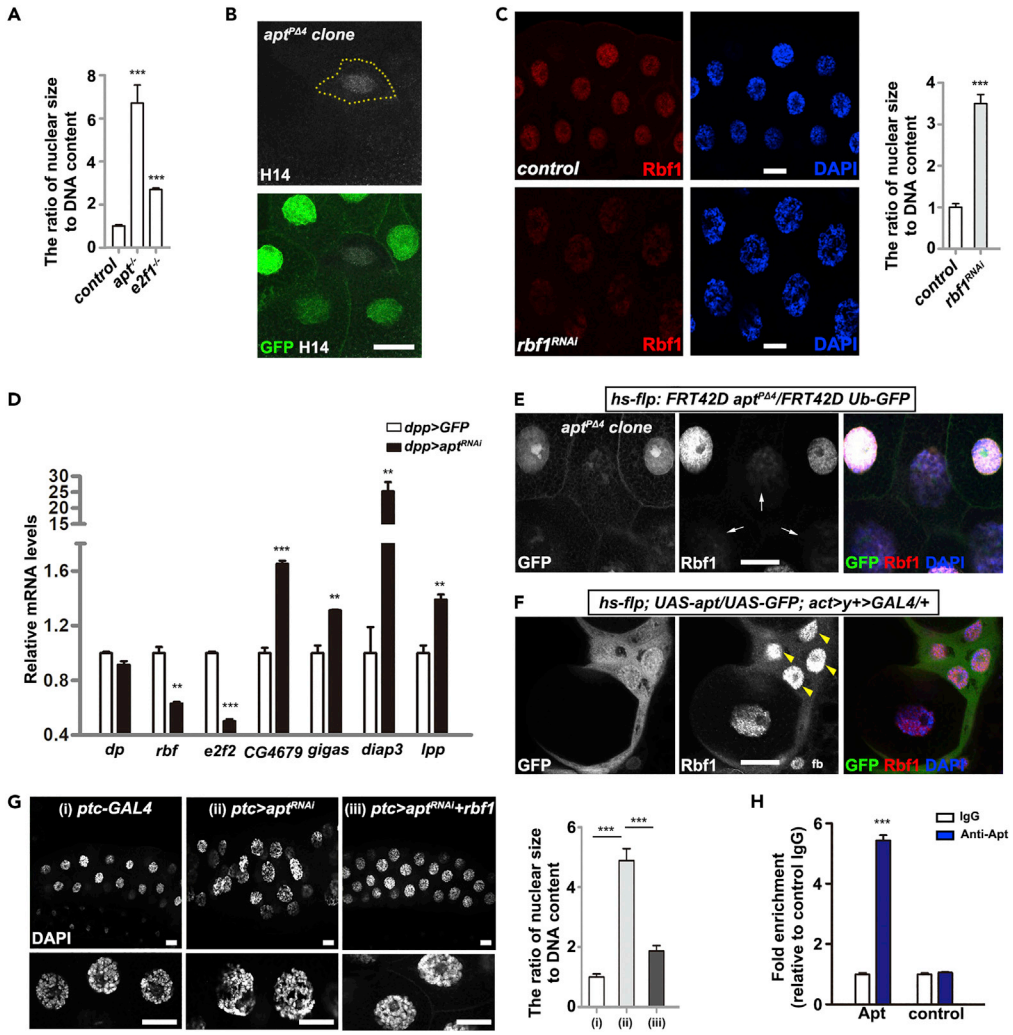


**Figure 4. Apt Regulates Chromatin Compaction through *rbf1* in the Salivary Gland**

(A) The ratio of nuclear size to DNA content in *apt*-mutant clone cells, *e2f1*-mutant clone cells, or control cells. Data were presented as mean ± SD. n = 10 for control, 4 for *apt*-mutant clone, and 3 for *e2f1*-mutant clone. ***p < 0.001 versus the control (Student's t test).

(B) Immunostaining of control or *apt*-mutant clone cells with the antibody against transcribing RNA polymerase II (H14). An *apt*-mutant clone cell (marked by yellow dotted line) showed prominent signals of transcribing RNA polymerase II compared with control cells. n = 3 with all samples showing the represented phenotype. Scale bar, 20 μm.

(C) *ptc-GAL4*-driven RNAi knockdown of *rbf1* induces de-compaction of chromatin. Compared with control cells, *rbf1*-knockdown cells exhibited larger nuclei with de-compacted chromatin. n = 10 with all samples showing the represented phenotype. Scale bars, 20 μm. Graph shows the ratio of nuclear size to DNA content. Data were mean ± SD relative to control. n = 100 for control and 100 for *rbf1* RNAi. The control samples were normalized to 1. ***p < 0.001 (Student's t test).

(D) RT-qPCR assays for the expression of *dp*, *rbf*, *e2f2,* and Rbf1-target genes (*CG4679*, *gigas*, *diap3*, *lpp*) in *dpp > GFP* control and *dpp* > GAL4-driven *apt*-knockdown salivary glands. Data were average ±SD relative to the *dpp > GFP* mRNA level. *dpp > GFP* samples were normalized to 1. **p < 0.01, ***p < 0.001 (Student's t test).

(E) The expression of Rbf1 in *apt*-mutant clone cells. Arrows indicate the decreased expression of Rbf1 in the clone. n = 4 with all samples showing the represented phenotype. Scale bar, 20μm.

(F) Up-regulation of Rbf1 in *apt*-overexpression cells. Yellow arrowheads indicate $y^+$-flipped out cells expressing *actin-GAL4* that drives overexpression of *apt*. n = 4 with all samples showing the represented phenotype. Scale bar, 20 μm. fb, fat body.

(G and H) (G) Chromatin de-compaction upon *ptc-Gal4*-driven RNAi of *apt* was suppressed by simultaneous overexpression of Rbf1. Upper panels are low-magnification images. Lower panels show higher-magnification images of the nuclei. n = 10 with all samples showing the represented phenotype. Scale bars, 20 μm. Graph shows the ratio of nuclear size to DNA content. Data were mean ± SD relative to control. n = 100 for control, 100 for *apt* RNAi, and 100 for

**Figure 4. *Continued***
apt RNAi + Rbf1 overexpression. The control samples were normalized to 1. ***p < 0.001 (Student's *t*-test). (H) ChIP assays showed occupancy of Apt on its binding motif at 156 nucleotides upstream of the transcription start site of *rbf1*. A control region was set around 500 nucleotides downstream of the Apt-binding motif. Data were presented as mean ± SD. n = three biological replicates. ***p < 0.001 versus the control (Student's t test). See also Figure S5.

knockdown and overexpression of *apt* induced cell migration and apoptosis, respectively, in the wing disc, which hampered inspection of the nuclear defects. Therefore, we employed mild knockdown or overexpression of *apt* that was triggered by heat shock-induced flipping out of $y^+$ from *actin* > $y^+$>*GAL4*. RNAi knockdown of *apt* reduced the Rbf1 expression (Figure 5A) and slightly increased the nuclear size/DNA ratio in wing disc cells (Figure 5B). Conversely, overexpression of Apt enhanced the Rbf1 expression (Figure 5C) and reduced the nuclear size/DNA ratio (Figure 5D). These results indicate that Apt up-regulates Rbf1 to direct proper chromatin compaction in wing disc cells also. Collectively, these data suggest that Apt-mediated CycE induction and chromatin compaction are general mechanisms common to both mitotic cycling and endocycling cells.

### Mutual Activation of *FSBP* and *E2f1*, and FSBP-Mediated Chromatin Compaction in Mammalian Cells

As Apt, E2f1, and Rbf1 are evolutionarily conserved transcription factors, the aforementioned mechanisms could be also conserved in mammalian cells. To test the possibility, we focused on the mammalian homologs of these factors, FSBP, E2f1, and Rb. In mouse NIH3T3 cells, RNAi knockdown of *FSBP* significantly decreased the expression of *E2f1* and *CycE* homologs (*CCNE1* and *CCNE2*) (Figure 6A). Upon *E2f1* knockdown, the expression of *FSBP*, *CCNE1,* and *CCNE2* were attenuated (Figure 6A). These data indicate mutual activation between *FSBP* and *E2f1* and requirement of *FSBP* and *E2f1* for the expression of *CCNEs*. In addition, knockdown of *FSBP* reduced the expression of *Rb1*, whereas overexpression of *FSBP* increased the *Rb1* expression (Figure 6B). Consistently, the target genes of Rb (*CDC6* and *DHFR*) also showed up- and down-regulation in *FSBP*-knockdown and *FSBP*-overexpressing cells, respectively (Figure 6B). These data indicate FSBP-mediated up-regulation of Rb. Furthermore, each *FSBP*-knockdown cell exhibited a large nucleus with less compact chromatin and a lower Rb protein level than the control cell did (Figures 6C–6E). Taken together, these results demonstrate Apt- and FSBP-mediated conserved mechanisms for CycE induction and chromatin compaction.

## DISCUSSION

This study revealed Apt-mediated up-regulation of two key players in the cell cycle, CycE and Rbf1. What is the significance of this finding? The positive feedback between *apt* and *e2f1* ensures rapid and robust induction of CycE at S phase entry. Apt also up-regulates Rbf1, but Rbf1 is inactivated through phosphorylation with Cdk2. After initiation of S phase, Rbf1 becomes active through de-phosphorylation and represses *cycE* (Du et al., 1996; Edgar and Orr-Weaver, 2001; van den Heuvel and Dyson, 2008). Together with $Crl4^{Cdt2}$-mediated degradation of E2f1 (Zielke et al., 2011), this leads to a rapid decline of CycE. Therefore, Apt governs both induction and subsequent repression of *cycE* with the aid of the periodic phosphorylation and de-phosphorylation of Rbf1.

E2f, a heterodimer of E2f1 and Dp, has been studied for many years, and it is a key regulator of CycE expression for S phase entry (Duronio et al., 1995). However, residual S phase takes place in a null mutant of *Drosophila e2f1* or *dp* (Duronio et al., 1998; Royzman et al., 1997). Here, we solved the discrepancy: another factor Apt also participates in the activation of *cycE*. Until this study, contribution of "another factor" if any was thought to be rather trivial compared with that of E2f, because *e2f1* or *dp* mutation severely reduced the CycE expression. Our study revealed that the notion is not correct. As Apt and E2f1 up-regulate each other and both Apt and E2f1 are required for the *cycE* expression, disruption of *e2f1* or *dp* function leads to depletion of both E2f and Apt, which in turn causes a severe defect in *cycE* expression. This masked the contribution of "another factor" Apt. Actually, transgenic reporter assays indicated that both the Apt-binding sites and the E2f1-binding sites in the regulatory region of *cycE* are necessary for the normal level of *cycE* transcription.

*apt*-Mutant cells induced in the salivary gland exhibited abnormal nuclei. The size of nucleus/DNA content was ~6.5 times higher than that of control cells, which resulted in de-compacted chromatin. Our study suggests that the unusual phenotype is due to release from Rbf1-mediated chromatin compaction and

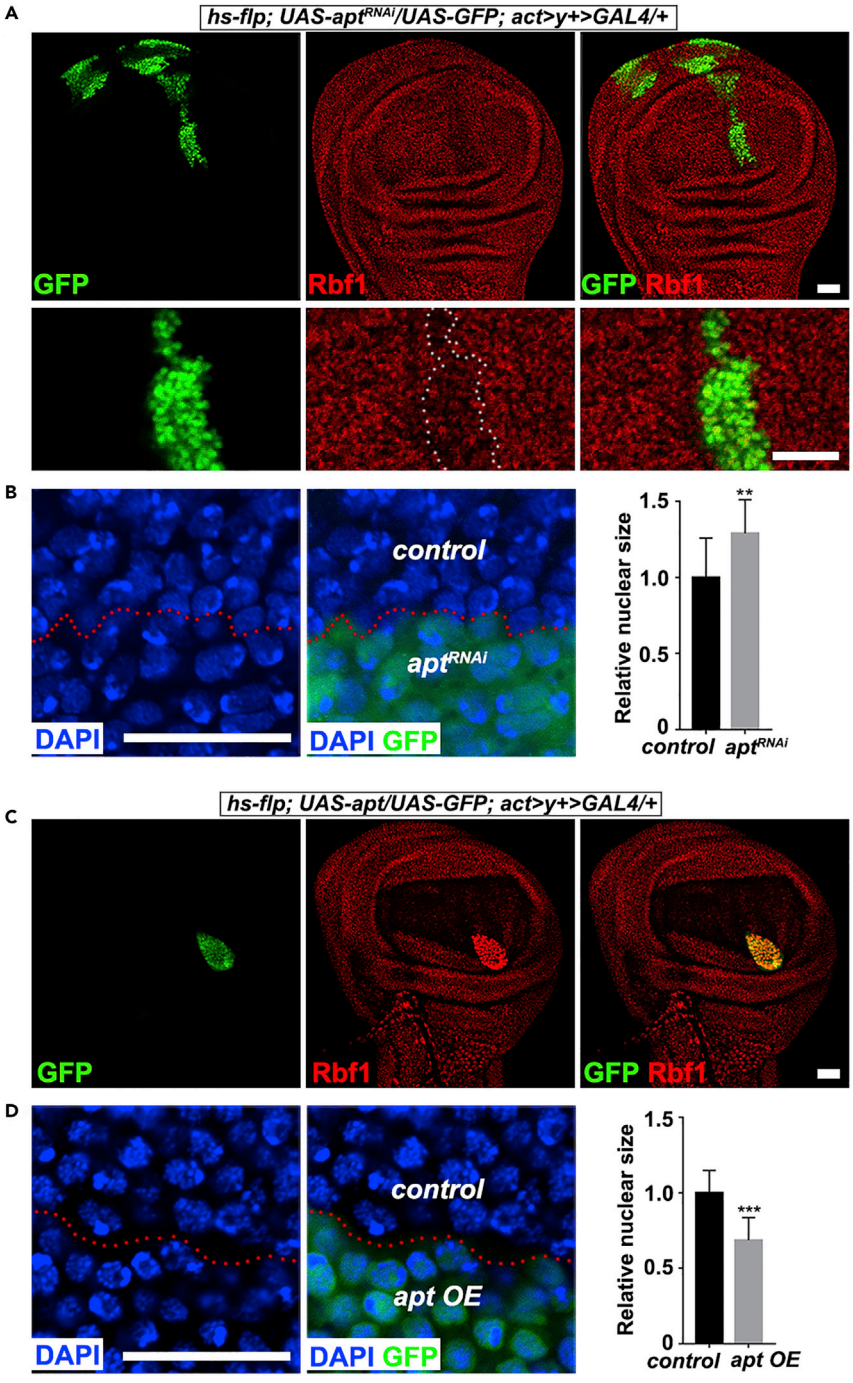


**Figure 5. Apt Regulates the Expression of Rbf1 and Chromatin Compaction in the Wing Disc**

(A) Immunostaining of a wing disc harboring *apt*-knockdown clones with anti-Rbf1 antibody (red). GFP (green) represents the region of $y^{+}$-flipped out *apt*-knockdown cells. n = 20 with all samples showing the represented phenotype. Lower panels are close-up images around the *apt*-knockdown clone. Scale bars, 20 μm.

(B) The wing disc nuclei of control cells (without GFP) and *apt*-knockdown cells (with GFP) were stained with DAPI. n = 3 with all samples showing the represented phenotype. Red dotted line indicates the boundary between control cells and *apt*-knockdown cells. Scale bar, 20 μm. Graph shows the ratio of nuclear size to DNA content in the control or *apt*-RNAi cells. Data were mean ± SD relative to control. n = 55 for control and 32 for *apt*-RNAi. The control samples were normalized to 1. **$p < 0.01$ (Student's t test).

**Figure 5. *Continued***

(C) Immunostaining of a wing disc harboring *apt*-overexpression cells with anti-Rbf1 antibody (red). GFP (green) implies the $y^+$-flipped out *apt*-overexpressing region. n = 25 with all samples showing the represented phenotype. Scale bar, 20 μm.

(D) The wing disc nuclei of control cells (without GFP) and *apt*-overexpression cells (with GFP) were stained with DAPI. n = 3 with all samples showing the represented phenotype. Red dotted line indicates the boundary between control cells and *apt*-overexpression cells. Scale bar, 20 μm. Graph shows the ratio of nuclear size to DNA content. Data were mean ± SD relative to control. n = 40 for control and 52 for *apt*-overexpression. The control samples were normalized to 1. ***p < 0.001 (Student's t test).

de-repression of Rbf1-target genes that occupy many loci throughout the genome (Korenjak et al., 2012). The nuclear size/DNA content of *e2f1*-mutant cells was also higher than that of control cells. However, the difference was less prominent than that between *apt*-mutant cells and control cells. We surmise the following explanation for it. Within a cell, there might exist a balance between the amounts of the E2f1/Dp complex and those of the Rbf1/E2f2/Dp complex. In *e2f1*-mutant cells, the level of the latter complex would increase in the absence of the former complex. This would compensate the decrease in Rbf1 and E2f2 due to reduced Apt, and would direct toward chromatin compaction.

This study underscores the importance of FSBP, a hitherto not-well-characterized transcription factor. Here we found FSBP- and Apt-mediated up-regulation of Rb and Rbf1, respectively. This raises an intriguing possibility that FSBP (Apt) suppresses tumor metastasis through up-regulation of Rb (Rbf1). Future studies should address the issue experimentally.

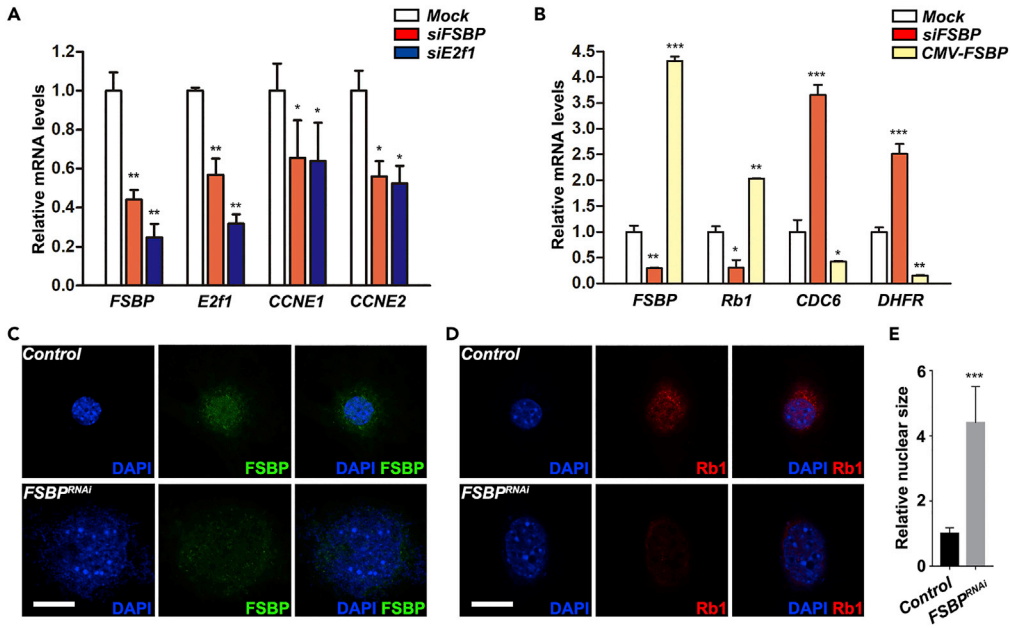


**Figure 6. Mutual Activation between *FSBP* and *E2f1*, and FSBP-Mediated Chromatin Compaction in Mouse NIH3T3 Cells**

(A) RT-qPCR assays for relative mRNA levels of *FSBP*, *E2f1*, *CCNE1*, and *CCNE2* in *FSBP*-knockdown cells or *E2f1*-knockdown cells. Data were mean ± SD relative to *Mock*. *p < 0.05, **p < 0.01 (Student's t test).

(B) Relative mRNA levels of *FSBP*, *Rb1*, *CDC6*, and *DHFR* from *FSBP*-knockdown cells or ectopic FSBP-expressing cells. Data were mean ± SD relative to *Mock*. *p < 0.05, **p < 0.01, ***p < 0.001 (Student's t test).

(C) Control and *FSBP*-knockdown cells were stained with DAPI (blue) and anti-FSBP antibody (green). n = 81 cells for control and 25 cells for *FSBP* knockdown with all samples showing the represented phenotype. Scale bar, 20 μm.

(D) Control and *FSBP*-knockdown cells were stained with DAPI (blue) and anti-Rb1 antibody (red). n = 85 cells for control and 26 cells for *FSBP* knockdown with all samples showing the represented phenotype. Scale bar, 20 μm.

(E) Quantification of the nuclear size. Data were mean ± SD relative to *Mock*. n = 16 for control and 6 for FSBP RNAi. ***p < 0.001 (Student's t test).

### Limitation of the Study

We demonstrate here Apt-dependent up-regulation of *rbf1*. There exists a single Apt-binding motif at 156 nucleotides upstream of the transcription start site of *rbf1*. ChIP assays showed occupancy of Apt on the motif. Therefore, it is most likely that Apt directly activates *rbf1* transcription through the binding site. However, further functional analyses including disruption of the Apt-binding site are necessary to verify the possibility.

### Resource Availability

#### *Lead Contact*

Further information and requests for resources and reagents should be directed to and will be fulfilled by the Lead Contact, Susumu Hirose (shirose@nig.ac.jp).

#### *Material Availability*

This study did not generate new materials.

#### *Data and Code Availability*

This study did not generate new datasets.

## METHODS

All methods can be found in the accompanying Transparent Methods supplemental file.

## SUPPLEMENTAL INFORMATION

Supplemental Information can be found online at https://doi.org/10.1016/j.isci.2020.101369.

## ACKNOWLEDGMENTS

We are grateful to Yash Hiromi for critical reading of the manuscript. We thank Yoichiro Tamori, Nicholas Dyson, Denise Montell, Vienna *Drosophila* Resource Center, Fly Stocks of National Institute of Genetics, and Bloomington Stock Center for kindly providing fly lines and reagents. We also thank Shu Kondo and the people in E.S.'s lab for discussions and suggestions. This work was supported by grants from the Japan Society for the Promotion of Science to E.S. (JSPS KAKENHI JP16F16703), the National Key Research and Development Program of China (2017YFE0129800), the National Natural Science Foundation of China (31872971 and 31571502), Funds of "Shandong Double Tops" Program (SYL2017YSTD09), and the Construction Engineering Special Fund of "Taishan Scholars" (no. ts201712022) to Q.-X.L. X.-F.W. was a postdoctoral fellow of JSPS.

## AUTHOR CONTRIBUTIONS

X.-F.W., Q.-X.L., S.H., and E.S. designed the project. S.H. and Q.-X.L. supervised the study. X.-F.W. performed the majority of the experiments and analyzed the data with the following exceptions. J.-X.L. and Z.-Z.Z. did the *in vitro* cell culture experiments and data analysis. Z.-Y.M. helped with the injection to prepare the transgenic flies. Y.S. and H.-R.Z. helped with a part of the genetic and staining experiments. X.-F.W. wrote the original draft. S.H. and Q.-X.L. revised the manuscript.

## DECLARATION OF INTERESTS

The authors declare no conflict of interest.

Received: February 6, 2020
Revised: May 24, 2020
Accepted: July 11, 2020
Published: August 21, 2020

## REFERENCES

Brehm, A., Miska, E.A., McCance, D.J., Reid, J.L., Bannister, A.J., and Kouzarides, T. (1998). Retinoblastoma protein recruits histone deacetylase to repress transcription. Nature *391*, 597–601.

Cayirlioglu, P., Ward, W.O., Silver Key, S.C., and Duronio, R.J. (2003). Transcriptional repressor functions of Drosophila E2F1 and E2F2 cooperate to inhibit genomic DNA synthesis in ovarian follicle cells. Mol. Cell Biol. *23*, 2123–2134.

De Veylder, L., Beeckman, T., Beemster, G.T., de Almeida Engler, J., Ormenese, S., Maes, S., Naudts, M., Van Der Schueren, E., Jacqmard, A., Engler, G., et al. (2002). Control of proliferation, endoreduplication and differentiation by the Arabidopsis E2Fa-DPa transcription factor. EMBO J. *21*, 1360–1368.

Du, W., Vidal, M., Xie, J.E., and Dyson, N. (1996). RBF, a novel RB-related gene that regulates E2F activity and interacts with cyclin E in Drosophila. Genes Dev. *10*, 1206–1218.

Dulic, V., Lees, E., and Reed, S.I. (1992). Association of human cyclin E with a periodic G1-S phase protein kinase. Science *257*, 1958–1961.

Duronio, R.J., Bonnette, P.C., and O'Farrell, P.H. (1998). Mutations of the Drosophila dDP, dE2F, and cyclin E genes reveal distinct roles for the E2F-DP transcription factor and cyclin E during the G1-S transition. Mol. Cell Biol. *18*, 141–151.

Duronio, R.J., O'Farrell, P.H., Xie, J.E., Brook, A., and Dyson, N. (1995). The transcription factor E2F is required for S phase during Drosophila embryogenesis. Genes Dev. *9*, 1445–1455.

Edgar, B.A., and Orr-Weaver, T.L. (2001). Endoreplication cell cycles: more for less. Cell *105*, 297–306.

Eulenberg, K.G., and Schuh, R. (1997). The tracheae defective gene encodes a bZIP protein that controls tracheal cell movement during Drosophila embryogenesis. EMBO J. *16*, 7156–7165.

Gellon, G., Harding, K.W., McGinnis, N., Martin, M.M., and McGinnis, W. (1997). A genetic screen for modifiers of Deformed homeotic function identifies novel genes required for head development. Development *124*, 3321–3331.

Jones, L., Richardson, H., and Saint, R. (2000). Tissue-specific regulation of cyclin E transcription during Drosophila melanogaster embryogenesis. Development *127*, 4619–4630.

Knoblich, J.A., Sauer, K., Jones, L., Richardson, H., Saint, R., and Lehner, C.F. (1994). Cyclin E controls S phase progression and its down-regulation during Drosophila embryogenesis is required for the arrest of cell proliferation. Cell *77*, 107–120.

Korenjak, M., Anderssen, E., Ramaswamy, S., Whetstine, J.R., and Dyson, N.J. (2012). RBF binding to both canonical E2F targets and noncanonical targets depends on functional dE2F/dDP complexes. Mol. Cell Biol. *32*, 4375–4387.

Lau, K.F., Perkinton, M.S., Rodriguez, L., McLoughlin, D.M., and Miller, C.C. (2010). An X11alpha/FSBP complex represses transcription of the GSK3beta gene promoter. Neuroreport *21*, 761–766.

Lie, Y.S., and Macdonald, P.M. (1999). Apontic binds the translational repressor Bruno and is implicated in regulation of oskar mRNA translation. Development *126*, 1129–1138.

Lilly, M.A., and Spradling, A.C. (1996). The Drosophila endocycle is controlled by Cyclin E and lacks a checkpoint ensuring S-phase completion. Genes Dev. *10*, 2514–2526.

Liu, Q.X., Jindra, M., Ueda, H., Hiromi, Y., and Hirose, S. (2003). Drosophila MBF1 is a co-activator for Tracheae Defective and contributes to the formation of tracheal and nervous systems. Development *130*, 719–728.

Liu, Q.X., Wang, X.F., Ikeo, K., Hirose, S., Gehring, W.J., and Gojobori, T. (2014). Evolutionarily conserved transcription factor Apontic controls the G1/S progression by inducing cyclin E during eye development. Proc. Natl. Acad. Sci. U S A *111*, 9497–9502.

Monahan, A.J., and Starz-Gaiano, M. (2016). Apontic regulates somatic stem cell numbers in Drosophila testes. BMC Dev. Biol. *16*, 5.

Nielsen, S.J., Schneider, R., Bauer, U.M., Bannister, A.J., Morrison, A., O'Carroll, D., Firestein, R., Clearly, M., Jenuwein, T., Herrera, R.E., and Kouzarides, T. (2001). Rb targets histone H3 methylation and HP1 to promoters. Nature *412*, 561–565.

Royzman, I., Whittaker, A.J., and Orr-Weaver, T.L. (1997). Mutations in Drosophila DP and E2F distinguish G1-S progression from an associated transcriptional program. Genes Dev. *11*, 1999–2011.

Shen, Y., Wang, L., Hirose, S., Zhou, Z., and Liu, Q. (2018). The transcriptional factor Apt regulates neuroblast differentiation through activating CycE expression. Biochem. Biophys. Res. Commun. *499*, 889–894.

Starz-Gaiano, M., Melani, M., Wang, X., Meinhardt, H., and Montell, D.J. (2008). Feedback inhibition of Jak/STAT signaling by apontic is required to limit an invasive cell population. Dev. Cell *14*, 726–738.

Su, M.T., Venkatesh, T.V., Wu, X., Golden, K., and Bodmer, R. (1999). The pioneer gene, apontic, is required for morphogenesis and function of the Drosophila heart. Mech. Dev. *80*, 125–132.

Talluri, S., and Dick, F.A. (2012). Regulation of transcription and chromatin structure by pRB: here, there and everywhere. Cell Cycle *11*, 3189–3198.

Thurmond, J., Goodman, J.L., Strelets, V.B., Attrill, H., Gramates, L.S., Marygold, S.J., Matthews, B.B., Millburn, G., Antonazzo, G., Trovisco, V., et al. (2019). FlyBase 2.0: the next generation. Nucleic Acids Res. *47*, D759–D765.

van den Heuvel, S., and Dyson, N.J. (2008). Conserved functions of the pRB and E2F families. Nat. Rev. Mol. Cell Biol. *9*, 713–724.

Wang, X.F., Shen, Y., Cheng, Q., Fu, C.L., Zhou, Z.Z., Hirose, S., and Liu, Q.X. (2017). Apontic directly activates hedgehog and cyclin E for proper organ growth and patterning. Sci. Rep. *7*, 12470.

Weng, L., Zhu, C., Xu, J., and Du, W. (2003). Critical role of active repression by E2F and Rb proteins in endoreplication during Drosophila development. EMBO J. *22*, 3865–3875.

Woodhouse, E.C., Fisher, A., Bandle, R.W., Bryant-Greenwood, B., Charboneau, L., Petricoin, E.F., 3rd, and Liotta, L.A. (2003). Drosophila screening model for metastasis: semaphorin 5c is required for l(2)gl cancer phenotype. Proc. Natl. Acad. Sci. U S A *100*, 11463–11468.

Zielke, N., Kim, K.J., Tran, V., Shibutani, S.T., Bravo, M.J., Nagarajan, S., van Straaten, M., Woods, B., von Dassow, G., Rottig, C., et al. (2011). Control of Drosophila endocycles by E2F and CRL4(CDT2). Nature *480*, 123–127.

**iScience, Volume *23***

## Supplemental Information

# Evolutionarily Conserved Roles for Apontic in Induction and Subsequent Decline of Cyclin E Expression

**Xian-Feng Wang, Jin-Xiao Liu, Zhi-Yuan Ma, Yang Shen, Hao-Ran Zhang, Zi-Zhang Zhou, Emiko Suzuki, Qing-Xin Liu, and Susumu Hirose**

Document S1. Figures S1-S5, Tables S1-S4 and Transparent Methods.

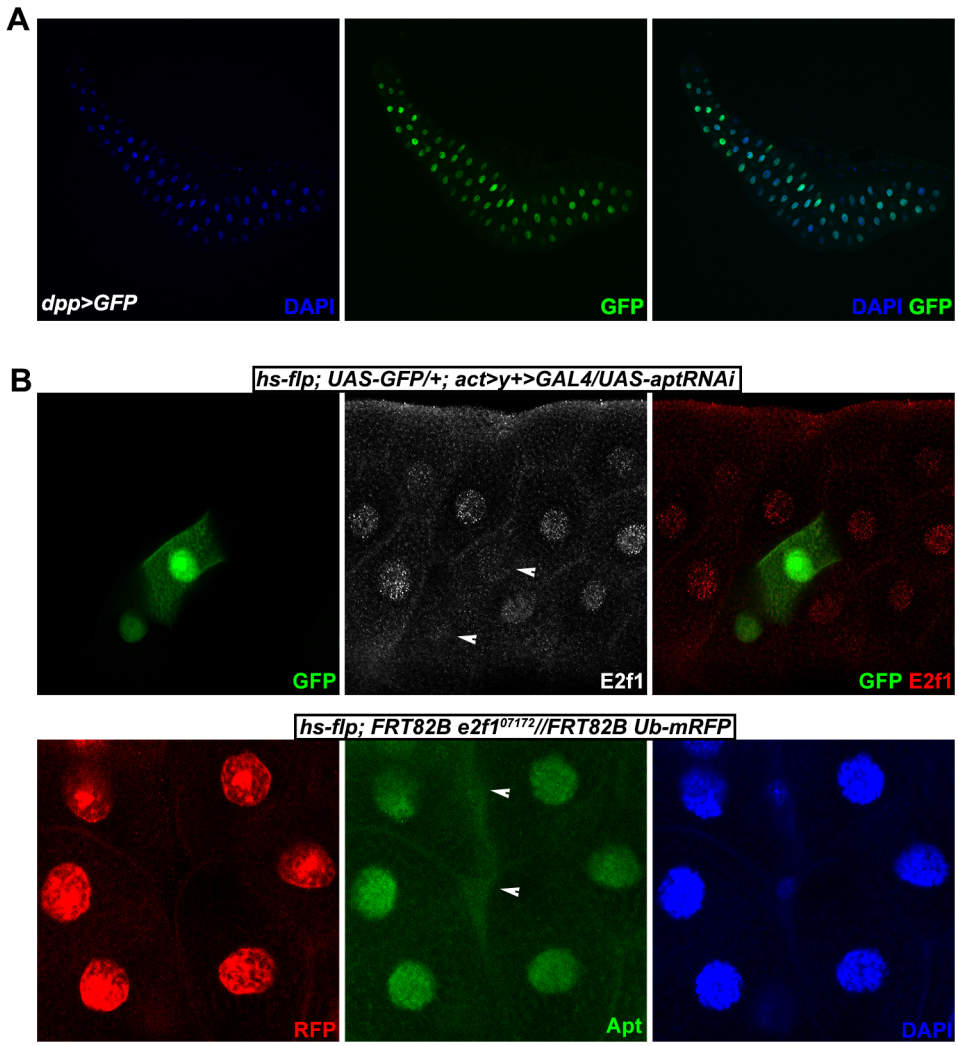


Figure S1. Supporting data for mutual activation of *apt* and *e2f1*, Related to Figure 1. (**A**) Expression of *dpp-GAL4* in the salivary gland. A *dpp>GFP* salivary gland stained with DAPI (blue) and anti-GFP antibody (green). (**B**) Expression of Apt and E2f1 depend on each other. Upper panels: A salivary gland carrying $apt^{RNAi}$ cells was stained with anti-E2f1 antibody. Arrowheads indicate significantly reduced expression of E2f1 in the *apt*-knockdown cells. Lower panels: A salivary gland carrying *e2f1*-mutant cells was stained with DAPI and anti-Apt antibody. Arrowheads indicate severely reduced expression of Apt in the *e2f1*-knockout cells

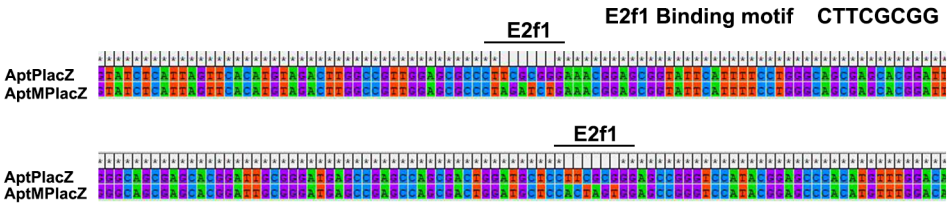


Figure S2. Sequence of the *apt* promoter region for reporter assays, Related to Figure 1.

AptPlacZ carries a control sequence with wild-type E2f1-binding sites. AptMPlacZ harbors mutated E2f1-binding sites.

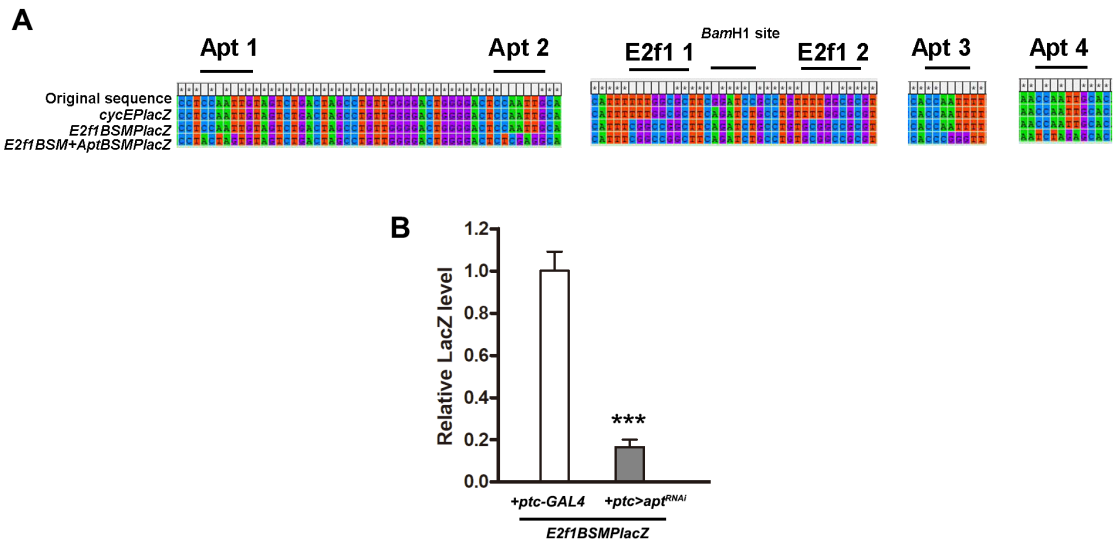


Figure S3. Reporter assays for *cycE* transcription, Related to Figure 3.

**(A)** Sequence in the *cycE* first intron for reporter assays. The original sequence contains a BamH1 enzyme site between the two E2f1-binding motifs. In order to use EcoR I and Bam HI for insertion into the vector, we disrupted the internal BamH1 site by base substitutions. *cycEPlacZ* is used for control. *E2f1BSMPlacZ* contains mutated E2f1-binding motifs. *E2f1BSM+AptBSMPlacZ* contains mutated E2f1- and Apt-binding motifs. (**B**) *ptc-GAL4*-driven RNAi knockdown of *apt* reduced the LacZ level in *E2f1BSMPlacZ***.** Data were mean ± SD relative to the level of *ptc-GAL4* control. n=20 for *ptc>apt*$^{RNAi}$ and 20 for *ptc-GAL4*. ***$P$<0.001.

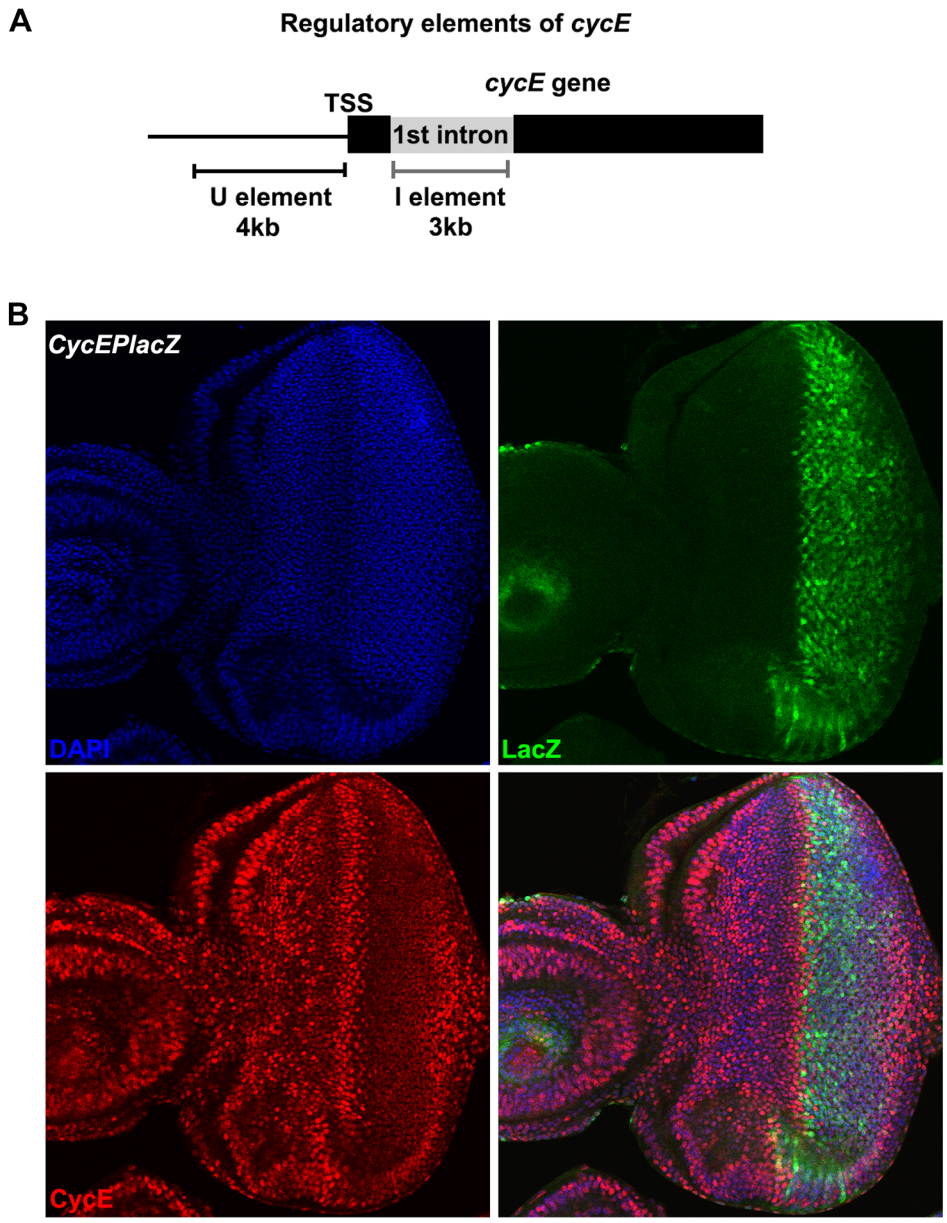


Figure S4. *cycE* regulatory elements, Related to Figure 3.

(**A**) Schematic presentation of the regulatory elements of *cycE*. U element: upstream region of *cycE* TSS. I element: intron (1st) region of *cycE*. TSS: transcription start site. (**B**) The eye disc from *cycEPlacZ* was stained with DAPI (blue), anti-LacZ antibody (green) and anti-CycE antibody (red).

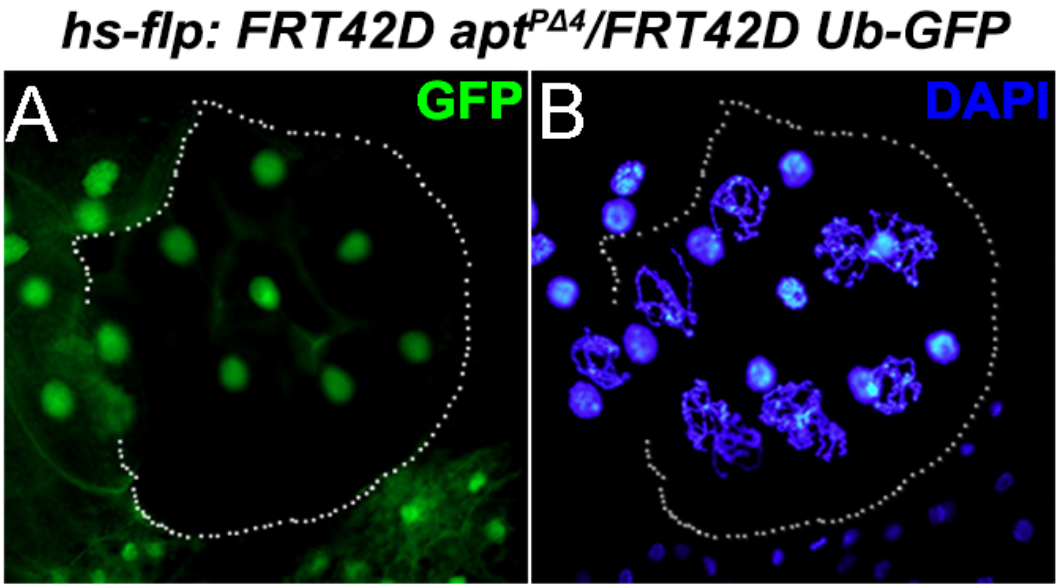


Figure S5. Higher magnification image of *apt* mutant nuclei, Related to Figure 4. *apt* mutant nuclei of the salivary gland (without GFP) exhibited intra-chromosomal chromatin de-compaction and large inter-chromosomal spaces compared with control nuclei (with GFP). Dotted line indicates an *apt* mutant clone.

**Table S1. Primers for RT-qPCR, Related to Figures 1, 4 and 6.**

apt-F: CGTCTCAGTGTGTCGCCTAA (Liu et al., PNAS, 2014)
apt-R: CGTGGCGGATATGTTGTTCA (Liu et al., PNAS, 2014)
e2f1-F: GCTCAACGTGGATCTCTTCA (Zielke et al., Nature, 2011)
e2f1-R: CGCCTTCACGTAAATCTCG (Zielke et al., Nature, 2011)
cycE-F: GCCATTCTTCCGAGTGATCT
cycE-R: GGCCATAAGCACTTCGTCAT
Dp-F: CCAAGGACAAGAAGGAGATT
Dp-R: ACGATGATGAACGGTAGC
Rbf-F: CGGCAACAAGGACACTAT
Rbf-R: CATCGTAGGCACTCAGAA
E2f2-F: CGGCTATGATGATGAAGGT
E2f2-R: GACTTGATTGGCGTTGGA
CG4679-F: AGTTCCAGATTCAGCATCC
CG4679-R: GCAGTTCGTCTACCTTCTT
Gigas-F: ATAATGTGGTGTCGCTGTT
Gigas-R: CCTCTGCTTCTGGTTCTG
Diap3-F: CAACGGAGAAGTGACCATT
Diap3-R: CCAGCGATAGGCAGTAGA
Ipp-F: AGGTGGATGTGTATCTGCTT
Ipp-R: CTCAATCAGGTACTTCAATGG
lacZ-F: CGAAGTGACCAGCGAATA
lacZ-R: GTAGTTCAGGCAGTTCAATC
tubulin 56D-F: GTTGACACTCGTTTAGCG (Nishioka et al., 2018, Development)
tubulin 56D-R: CCCAAGTATGGCTCTCAATA (Nishioka et al., 2018, Development)

FSBP-F: TTTCGGAGCCCACCAAGCAA
FSBP-R: GCAGTCTCATCCAAGTTTGC
CCNE1-F: GTGGCTCCGACCTTTCAGT
CCNE1-R: CACAGTCTTGTCAATCTTGGC
CCNE2-F: TCTGTGCATTCTAGCCATCG
CCNE2-R: ATCCAGTCTACACATTCCGAG
e2f1-mouse-F: AGAAACGGCGCATCTATGAC
e2f1-mouse-R: CTTCAAGCCGCTTACCAATC
rb1-F: TCTCACCTCCTGCACTACT
rb1-R: TGACCTCTTCTGGGTGTTCG
mcdc6-F: AATTGTGGAGTCGGATGTCAG
mcdc6-R: AAAGTCACCCTGTTCCCATC
mDHFR-F: CATGGTTTGGATAGTCGGAGG
mDHFR-R: GTCACAAAGAGTCTGAGGTGG
GAPDH-F: TGTGTCCGTCGTGGATCTGA
GAPDH-R: TGCTGTTGAAGTCGCAGGAG

**Table S2. Primers for ChIP, Related to Figures 3 and 4.**

E2f1BS-F: GCCACCAGCGGCTTCATCG
E2f1BS-R: CGGCGGCAGCAAAGTGATC
AptBS1-2-F: CTCGTCAGCTGTTTTTCGAC
AptBS1-2-R: GGCAAGCTTGGCATTTTATT
AptBS3-F: GCCACCAGCGGCTTCATCG (same as E2f1BS)
AptBS3-R: CGGCGGCAGCAAAGTGATC (same as E2f1BS)
AptBS4-F: TGATACCCAGTTCCACCA
AptBS4-R: CAAAGACACGACGGCAAA

E2f1BS-Ctr1-F: CTTGCGATCATTGTGTTACT
E2f1BS-Ctr1-R: GGACTGGAATGGTGATGAA
E2f1BS-Ctr2-F: AATGAGTGAGCGAGATAGAC
E2f1BS-Ctr2-R: AAGCAGAGGAGAAGAGGAA
AptBS-Ctr1-F: AATGAGTGAGCGAGATAGAC (same as E2f1BS-Ctr2-F)
AptBS-Crt1-R: AAGCAGAGGAGAAGAGGAA (same as E2f1BS-Ctr2-R)
AptBS-Ctr2-F: AACTCCGACTCTCTCTTTGC
AptBS-Ctr2-R: AAGTGGCACTGTGACGAGAT

**Table S3. Primers for reporter assays, Related to Figures 1 and 3.**

apt promoter

Reporter-AptF: GGAATTCCCTATAATCGCCATTAGTC (EcoRI )

Reporter-AptR: CGGGATCCCGTTACTGTATAAGCTAT (BamHI)

E2F11-AptR: GAAGATCTAGGGCGCTCCAACGGCCA

E2F11-AptF: GAAGATCTGAAACGGAGCGGTATTCA

E2F12-AptR: GACTAGTGGAGCATCCAGTCGCTGGCT

E2F12-AptF: GACTAGTGGAGCCGGGTCCATACGGA

cycE promoter

Reporter-cycE-F: GGAATTCGCAGTCGAAAAGTAATGGAA (EcoRI )

Reporter-cycE-R: CGGGATCCAATCCTTTGATGACATACCGCT (BamHI)

Bamh1-R1: CGGCTAGCGAAGCGCCAAAAAATGCAACA

Bamh1-F1: CGGCTAGCGCCTGTTTTGGCGCGTTCCTCAT

Apt1-R: GACTAGTAGGTTCGACGTCCAGTCAG

Apt1-F: GACTAGTGTAGTCTGACTAGCCTGTT

Apt2-R: CCCTCGAGAGTCCCCAGTCCCCAACAGGCTA

Apt2-F: CCCTCGAGGCAGACTCCATTCAATAAAATG

E2f11-R: CCCGGCCGAAATGCAACAAACACAGGGG

E2f11-F: CCCGGCCGGCTTCGCTAGCGCCTGTTTT

E2f12-R: ATTTGCGGCCGCACAGGCGCTAGCGAAGCG

E2f12-F: ATTTGCGGCCGCGTTCCTCATGCACACTCG

Apt3-R: CCCCCGGGTGGAACTGGGTATCAAAAGCA

Apt3-F: CCCCCGGGTTTTTTTCGGTTCCAAAGCGAT

Apt4-R: GCTCTAGATTTTACCTTCTAGTAAGCGGA

Apt4-F: GCTCTAGAGCACAATGGTTTTAGTGGATA

**Table S4. Example for measurement, Related to Figure 2B**

| **Round 1** | Area | | Mean | **Relative Intensity** |
|---|---|---|---|---|
| mutant 1 | 0.034 | | 1440.647 | 0.180248168 |
| Ctr1 for mutant 1 | 0.022 | | 6003.591 | 0.751146032 |
| Ctr2 for mutant 1 | 0.018 | | 8622.778 | 1.078848556 |
| Ctr3 for mutant 1 | 0.018 | | 8647 | 1.081879119 |
| Ctr4 for mutant 1 | 0.02 | | 7215.8 | 0.902812923 |
| Ctr5 for mutant 1 | 0.017 | | 9473.706 | 1.185313369 |
| | | average of Round 1 control | 7992.575 | |

| **Round 2** | Area | | Mean | **Relative Intensity** |
|---|---|---|---|---|
| mutant 2 | 0.051 | | 1126.627 | 0.108180336 |
| mutant 3 | 0.035 | | 1464.314 | 0.140605525 |
| mutant 4 | 0.028 | | 1865.071 | 0.179086786 |
| Ctr1 for mutant 234 | 0.021 | | 8297.333 | 0.796721786 |
| Ctr2 for mutant 234 | 0.017 | | 10448.06 | 1.003237574 |
| Ctr3 for mutant 234 | 0.015 | | 12161.47 | 1.167761461 |
| Ctr4 for mutant 234 | 0.015 | | 12595.4 | 1.209428329 |
| Ctr5 for mutant 234 | 0.02 | | 8569.45 | 0.82285085 |
| | | average of Round 2 control | 10414.34 | |

| **Control** | **mutant** (relative to control) |
|---|---|
| 0.751146 | 0.180248 |
| 1.078849 | 0.10818 |
| 1.081879 | 0.140606 |
| 0.902813 | 0.179087 |
| 1.185313 | |
| 0.796722 | |
| 1.003238 | |
| 1.167761 | |
| 1.209428 | |
| 0.822851 | |

## Transparent Methods

### Fly strains

*Drosophila* lines were raised in a cornmeal-based regular fly medium (Kayashima et al., 2005). *hsFlp*; *FRT42D*, *Ubi-GFP* and *FRT42D*, $apt^{P\Delta 4}$ have been described (Wang et al. , 2017). *hsFlp*; *FRT 82B*, *Ubi-mRFP* and *FRT 82B* lines were gifts from Dr. Tamori. *e2f1* mutants, $e2f1^{07172}$ (BDSC: 11717) and $e2f1^{rm729}$ (BDSC: 35849), *dpp-GAL4* (BDSC: 7006), *UAS-GFP* (BDSC: 35544), *ptc-GAL4* (BDSC: 81616), *UAS-rbf1* (BDSC: 50746) and *UAS-rbf1*RNAi (BDSC: 36744) were obtained from Bloomington Drosophila Stock Center. *UAS-apt*RNAi (VDRC: v4289) and *UAS-e2f1*RNAi (NIG-fly: HMS01541) were from Vienna Drosophila Resource Center and Fly Stocks of National Institute of Genetics, respectively. The fly of *FRT 82B*, $e2f1^{07172}$*/TM6B* was established through recombination. To induce mutant clones of *apt* or *e2f1*, 2-6 hours AEL embryos were heat shocked at 37 °C for 40 minutes and then reared at 25 °C. *UAS-apt* was a gift from Dr. Montell. *hsFLP*; *act>y+>GFP* (*Ay-GLA4*) was a gift from Dr. Tamori and the flip-out cells were induced by a 12-minutes heat shock to second instar larvae.

### Immunohistochemistry and Confocal Imaging

Salivary glands or discs were dissected in phosphate buffered saline (PBS), fixed in 4% formaldehyde in PBS for 20 minutes. After washing with PBS with 0.1% Triton X-100, the samples were stained with antibodies in the same solution. We incubated samples with primary antibodies at 4°C for overnight with shaking, and then washed samples for 15 minutes three times. Primary antibodies were used at following dilutions: Rabbit

anti-Apt (1:1000); goat anti-E2f1 (1:100, Aviva Systems Biology, OAEB03032); goat anti-CycE (1:200, Santa Cruz, sc-15903); mouse anti-LacZ (1:500, DSHB, 40-1a); mouse anti-Rbf1 (1:50, a gift from Dr. Dyson); mouse anti-H14 (1:100, Covance, 920304); rabbit anti-FSBP (1:500, ATLAS ANTIBODIES, HPA025059); rabbit anti-Rb1 (1:200, ABclonal, A11409). The secondary antibodies conjugated with Alexa 488 (Molecular Probes, R37114), Cy3 (Jackson ImmunoResearch, 711-165-152, 715-165-150, 705-167-003) and Cy5 (Jackson ImmunoResearch, 711-175-152, 715-175-150) were diluted 1:500 and incubated at room temperature for 2 hours. After washing, samples were mounted and imaged with an Olympus FV1200 Confocal Microscope.

**Image analysis**

For nuclear size and DNA content analysis, images from Confocal were quantified using Analyze function of the ImageJ software according to the reference (Zielke, et al., 2011). For the measurement of clone cells and their neighboring controls, we did z-stack using confocal sections. Nuclei that visually overlapped with their neighboring cells were not analyzed. Regions were selected using freeform selection tool. The area function was used to measure nuclear area. DNA content was quantified by DAPI mean grey value. An example of the measurement was shown in Table S4. Statistical analyses on LacZ expression, DNA content, nuclear size and nuclear size / DNA content data were carried out with Student's *t*-test.

**Motif search**

The regulatory sequences of *apt* and *cycE* were obtained from UCSC (http://genome.ucsc.edu). E2f1- and Apt-motifs were derived from published references (Kel et al., 2001; Korenjak et al., 2012; Liu et al., 2003; Yamaguchi et al., 1995). E2f1-binding motif used in this study was TTTGGCGC or CTTCGCGG. Apt-binding motif was (T)CCAATT(G).

**Chromatin immunoprecipitation (ChIP)**

ChIP experiments were performed as previously described (Wang et al., 2017). Briefly, 200 early third instar salivary glands were dissected, fixed, homogenized and sonicated. After analyzed the fragment sizes, sonicated samples were immunoprecipitated with antibodies. 2μl of purified DNA from ChIP samples and input were amplified using specific primers (Table S2). Statistical analyses on ChIP data were carried out with Student's *t*-test.

**Plasmid constructions and transgenic flies**

*AptPlacZ* was made by inserting a 1.5 kb *apt*-promoter region that contains E2f1-binding motifs into a CaSpeR-AUG-β-gal vector (Thummel et al., 1988). AptMPlacz with mutated E2f1-binding motifs was made from *AptPlacZ*. *cycEPlacZ* construct was made by inserting a 3 kb region in the first intron of *cycE* carrying Apt- and E2f1-binding motifs into a hsCaspeR-AUG-β-gal vector (Thummel et al., 1988). *E2fBSMPlacZ* with mutated E2f1-binding motifs and *E2fBSM+AptBSMPlacZ* with

mutated E2f1- and Apt-binding motifs were made from *cycEPlacZ*. Primers used for mutagenesis of the binding motifs are shown in Table S3. To generate transgenic fly lines, constructs were injected into the germ line. After chromosomal mapping, flies with normal *mini-w*$^{+}$ expression were used for reporter assays.

**RT-qPCR**

Total RNAs were prepared from 40 dissected early third instar salivary glands using an RNAprep kit (Zymo Research, Cat. number R2050). cDNAs were synthesized from RNA samples of three biological replicates. qPCR was performed as described previously (Wang et al., 2017). Primer sequences used for qPCR are shown in Table S1. The amount of mRNA was normalized to that of β-tubulin mRNA and then presented as fold change against the control mRNA level. Statistical analyses were performed by Student's *t*-test.

**Cell culture and transfection**

NIH3T3 cells were grown in Dulbecco's modified Eagle medium (Biological Industries, REF number 06-1055-57-1A) supplemented with 10% Fetal Bovine Serum (FBS) and 1% penicillin/streptomycin. To silence FSBP or E2f1, siRNAs were transfected at a final concentration of 100nM using lipofectamine 2000 (Invitrogen, Product number 11668019) according to the manufacturer's instruction. The siRNA sequences used were: Negative control: 5'-UUCUCCGAACGUGUCACGUdTdT; FSBP-siRNA: 5'-GCAAGUCAUGGAAAUGAUUTTdTdT; E2F1-siRNA:

5’-GGAUCUGGAGACUGACCAUTTdTdT. To generate Fg-mFSBP for mammalian cell expression, we amplified this gene via cDNA and cloned it into CMV-Fg constructs. The primer pairs used were as follows: mFSBP-Forward: 5’-ATGGTAGGAAAGGCTAGATC-3’ and mFSBP-Reverse: 5’-TCAGAGACTACTGTATTGAG-3’. Cells were harvested for RT-qPCR analyses as previously described (Wang et al., 2017). Primers used were shown in Table S1.

**Supplemental References**

Kayashima, Y., Hirose, S., Ueda, H. (2005) Anterior epidermis-specific expression of the cuticle gene *EDG84A* is controlled by many cic-regulatory elements in *Drosophila melanogaster*. Dev Genes Evol *215*, 545-552.

Kel, A.E., Kel-Margoulis, O.V., Farnham, P.J., Bartley, S.M., Wingender, E., Zhang, M.Q. (2001) Computer-assisted identification of cell cycle-related genes: new targets for E2F transcription factors. J Mol Biol *309*, 99-120.

Korenjak, M., Anderssen, E., Ramaswamy, S., Whetstine, J.R., Dyson, N.J. (2012) RBF binding to both canonical E2F targets and noncanonical targets depends on functional dE2F/dDP complexes. Mol Cell Biol *32*, 4375-87.

Liu, Q.X., Jindra, M., Ueda, H., Hiromi, Y., Hirose, S. (2003) *Drosophila* MBF1 is a co-activator for Tracheae Defective and contributes to the formation of tracheal and nervous systems. Development *130*, 719-28.

Liu, Q.X., Wang, X.F., Ikeo, K., Hirose, S., Gehring, W.J., Gojobori, T. (2014) Evolutionarily conserved transcription factor Apontic controls the G1/S progression by

inducing *cyclin E* during eye development. Proceedings of the National Academy of Sciences of the United States of America *111*, 9497-502.

Nishioka, K., Wang, X.F., Miyazaki, H., Soejima, H., Hirose, S. (2018) Mbf1 ensures Polycomb silencing by protecting *E(z)* mRNA from degradation by Packman. Development *145* dev162461.

Thummel, C.S., Boulet, A.M., Lipshitz, H.D. (1988) Vectors for *Drosophila* P-element-mediated transformation and tissue culture transfection. Gene *74*, 445-456.

Wang, X.F., Shen, Y., Cheng, Q., Fu, C.L., Zhou, Z.Z., Hirose, S., Liu, Q.X. (2017) Apontic directly activates hedgehog and *cyclin E* for proper organ growth and patterning. Sci Rep *7*, 12470.

Yamaguchi, M., Hayashi, Y., Matsukage, A. (1995) Essential role of E2F recognition sites in regulation of the proliferating cell nuclear antigen gene promoter during *Drosophila* development. J Biol Chem *270*, 25159-65.

Zielke, N., Kim, K.J., Tran, V., Shibutani, S.T., Bravo, M.J., Nagarajan, S., van Straaten, M., Woods, B., von Dassow, G., Rottig, C., Lehner, C.F., Grewal, S.S., Duronio, R.J., Edgar, B.A. (2011) Control of *Drosophila* endocycles by E2F and CRL4(CDT2). Nature *480*, 123-127.